

---

# Some aspects of a gradient damage formulation

**Tina Liebe\* – Paul Steinmann\* – Ahmed Benallal\*\***

*\* Chair for Applied Mechanics, Department of Mechanical Engineering,  
University of Kaiserslautern, P.O. Box 3049, D-67653 Kaiserslautern, Germany  
liebe@rhrk.uni-kl.de, ps@rhrk.uni-kl.de,  
mechanik.mv.uni-kl.de/*

*\*\* Laboratoire de Mécanique et Technologie, LMT-Cachan,  
61 avenue du Président-Wilson, F-94235 Cachan Cedex, France  
Ahmed.Benallal@lmt.ens-cachan.fr  
www.lmt.ens-cachan.fr/*

---

*ABSTRACT. The paper discusses some theoretical and numerical aspects of a gradient damage formulation. Thereby, the main motivation is provided by localization computations whereby classical local continuum formulations fail to produce physically meaningful and numerically converging results. Therefore, we propose a formulation in terms of the Helmholtz free energy incorporating the gradient of the damage field, a dissipation potential and the postulate of maximum dissipation. As a result the driving force conjugated to damage evolution incorporates besides the strictly local energy release rate essentially the divergence of a vectorial damage flux. At the numerical side, besides balance of linear momentum, the algorithmic consistency condition has to be solved in weak form.*

*RÉSUMÉ. Les aspects essentiels d'un modèle de rupture incorporant le gradient de l'endommagement sont discutés dans ce travail. Au niveau de la formulation, la particularité réside dans la définition de la variable thermodynamique conjuguée à l'endommagement. Celle-ci inclut en plus de la partie classique (taux de restitution d'énergie due à l'endommagement) une contribution prenant en compte la dissipation due au gradient d'endommagement. Du côté numérique, l'endommagement est considéré comme variable nodale indépendante et la condition de cohérence est traitée au niveau global. Les conséquences numériques de la formulation sont soulignées et illustrées sur des exemples simples.*

*KEYWORDS: Continuum Damage Mechanics, Gradient Regularization, Finite Element Method*

*MOTS-CLÉS: Continuum Damage Mechanics, Gradient Regularization, Finite Element Method*

---

## 1. Introduction

Softening at the continuum level due to damage accumulation mimics deterioration processes within the material at the micro scale. As a consequence of softening, damage tends to accumulate within narrow bands, so called localized zones. In experiments these localization zones display a finite width which is related to the micro structure of the material. Upon further loading localized zones then most often form a precursor to the final rupture of the material. In a standard continuum description and in particular in the corresponding numerical solution schemes no finite width is obtained, instead pathologically mesh dependent solutions are observed upon refinement of the discretization.

Among the most effective remedies against the unphysical behavior displayed by a softening standard continuum and its numerical computation nonstandard continuum theories have been proposed which incorporate higher gradients of those quantities which are responsible for softening. Physically motivated gradient models in crystal plasticity were proposed, e.g. by Steinmann [STE 96] and Menzel & Steinmann [MEN 00]. Gradient dependent models, whereby the gradient dependence is essentially incorporated in the loading surface by the Laplacian of an internal variable, were treated by e.g. Comi [COM 96], de Borst, Benallal & Heeres [BOR 96a], Benallal & Tvergaard [BEN 95]. The well-posedness of the initial boundary value problem for a continuum model was studied by Benallal, Billardon & Geymonat [BEN 93].

A variety of numerical strategies, different from the one proposed in this work, were investigated e.g. by Sluys, de Borst & Mühlhaus [SLU 93], Pamin [PAM 94], de Borst & Pamin [BOR 96b], Peerlings et. al [PEE 96], Steinmann [STE 99], Comi [COM 99].

In this contribution the essential ingredient of gradient damage is an additional equation represented by the damage condition containing the quasi-nonlocal energy release rate. A noteworthy feature from the numerical point of view is thus the treatment of the damage field as an independent variable.

## 2. A Gradient damage formulation

As a simple phenomenological measure of micro defect interactions we might consider the gradient of the damage field  $\mathbf{d} = \nabla_x d$ , which we include in the free Helmholtz energy  $\Psi = \Psi(d, \epsilon, \mathbf{d})$  of the standard local damage model. Moreover, the model is based on a dissipation potential and the postulate of maximum dissipation. Therefore healing processes are excluded and a thermodynamically consistent approach is envisioned. Thereby, due to the extension of the classical local theory with the damage gradient contribution, the local dissipation inequality  $\mathcal{D} = Y\dot{d} + \mathbf{Y} \cdot \dot{\mathbf{d}} + \mathcal{P} \geq 0$  for the whole body  $\mathcal{B}$  incorporates the nonlocality residual  $\mathcal{P}$ , which, according to the arguments by Polizzotto & Borino [POL 98] satisfies the insulation condition  $\int_{\mathcal{B}^d} \mathcal{P} dV = 0$  on the actively damaged part of the whole body

$$\Psi = \Psi(d, \epsilon, \mathbf{d}) = \Psi^{mac}(d, \epsilon) + \Psi^{grd}(\mathbf{d}) \quad (1)$$

$$\mathcal{D} = Y\dot{d} + \mathbf{Y} \cdot \dot{\mathbf{d}} + \mathcal{P} = \bar{Y}\dot{d} \geq 0 \quad (2)$$

$$\int_{\mathcal{B}^d} \mathcal{P} dV = 0 \quad \text{with} \quad \mathcal{P} = \bar{Y}\dot{d} - Y\dot{d} - \mathbf{Y} \cdot \dot{\mathbf{d}} \quad (3)$$

$$\boldsymbol{\sigma} = \boldsymbol{\sigma}(d, \epsilon) = \partial_{\epsilon} \Psi^{mac} \quad (4)$$

$$Y = Y(d, \epsilon) = -\partial_d \Psi^{mac} \quad (5)$$

$$\mathbf{Y} = \mathbf{Y}(\mathbf{d}) = -\partial_{\mathbf{d}} \Psi^{grd} \quad (6)$$

$$\bar{Y} = Y - \text{div} \mathbf{Y} \quad (7)$$

$$\mathbf{n} \cdot \mathbf{Y} = 0 \quad \text{on} \quad \partial \mathcal{B}_{ext}^d \subseteq \partial \mathcal{B} \quad (8)$$

$$\dot{d} = 0 \quad \text{on} \quad \partial \mathcal{B}_{int}^d \quad (9)$$

$$\varphi(\bar{Y}; \kappa) = \bar{Y} - \kappa \quad \text{with} \quad \kappa = \kappa(d) \quad (10)$$

$$\varphi(\bar{Y}; \kappa) \leq 0 \quad \dot{d} \geq 0 \quad \dot{d}\varphi = 0 \quad (11)$$

(1) Free Energy, (2) Dissipation Inequality, (3) Insulation Condition of Nonlocality Residual, (4) Macroscopic Stress, (5) Energy Release Rate, (6) Damage Flux, (7) Quasi-Nonlocal Energy Release Rate, (8) Constitutive Boundary Conditions, (9) Continuity Boundary Conditions, (10) Damage Condition, (11) Kuhn-Tucker Conditions

**Table 1.** Key Ingredients of Gradient Damage

$\mathcal{B}^d \subseteq \mathcal{B}$ . Thereby, the assumption of a bilinear form for the dissipation power  $\mathcal{D} = \bar{Y}\dot{d}$  determines the quasi-nonlocal energy release rate  $\bar{Y} = \bar{Y}(\epsilon, \mathbf{d}, d)$  as conjugated to the evolution of the independent arbitrary damage variable field in  $\mathcal{B}^d \subseteq \mathcal{B}$ . Moreover, applying the insulation condition, integration by parts and invoking Gauss theorem on the nonlocality residual yields a constitutive boundary condition (homogeneous Neumann b.c.) on  $\partial \mathcal{B}_{ext}^d \subseteq \partial \mathcal{B}$  for the vector field  $\mathbf{Y} = \mathbf{Y}(\mathbf{d})$  which is thermodynamically conjugated to the gradient of the damage variable  $\mathbf{d}$  and which we tend to denote the damage flux. In addition to that, it results also in the so-called continuity boundary condition  $\dot{d} = 0$ , which is imposed on  $\partial \mathcal{B}_{int}^d$  with  $\partial \mathcal{B}^d = \partial \mathcal{B}_{ext}^d \cup \partial \mathcal{B}_{int}^d$ . Thus, compatibility between the evolution of the damage variable and its gradient is automatically assured. The quasi-nonlocal energy release rate essentially contains the divergence of the damage flux  $\text{div} \mathbf{Y}$  in addition to the local energy release rate  $Y$ . Finally it can be stated that the damage condition and the Kuhn-Tucker conditions retain the same structure as for the local case. Therefore, we end up with a coupled problem for the two primary unknown fields  $\mathbf{x}$  and  $d$  which have to satisfy a partial differential equation and an inequality constraint simultaneously, as will be shown in the sequel. The key ingredients of our gradient damage formulation are summarized in Table 1.

### 3. Strong form of the coupled problem

To set the stage for the following developments we first summarize the pertinent set of equations for the solution of the coupled boundary value problem in strong form.

Let  $\mathcal{B}$  denote the configuration occupied by a solid body. Then the displacement field  $\mathbf{u} = \mathbf{u}(\mathbf{x})$  and the damage field  $d = d(\mathbf{x})$  are parameterized in terms of the placements  $\mathbf{x} \in \mathcal{B}$ . These two primary fields are determined by the simultaneous solution of a partial differential equation and a set of Kuhn-Tucker-complementary conditions. The boundary  $\partial\mathcal{B}$  to  $\mathcal{B}$  with outward normal  $\mathbf{n}$  is subdivided into disjoint parts whereby either Neumann or Dirichlet boundary conditions for the two solution fields  $\mathbf{u}(\mathbf{x})$  and  $d(\mathbf{x})$  are prescribed. The residua of the resulting coupled problem in strong form are displayed in Table 2.

$\mathbf{r}^u(\mathbf{u}, d) = 0$	(1)
$r^\varphi(\mathbf{u}, d) \leq 0 \quad \dot{r}^d(\dot{d}) \geq 0$	(2)
$\mathcal{B} = \mathcal{B}^e \cup \mathcal{B}^d \quad \text{and} \quad \emptyset = \mathcal{B}^e \cap \mathcal{B}^d$	(3)
$\mathcal{B}^e = \{\mathbf{x} \in \mathcal{B} \mid \varphi \leq 0, \dot{d} = 0\}$	(4)
$\mathcal{B}^d = \{\mathbf{x} \in \mathcal{B} \mid \varphi = 0, \dot{d} > 0\}$	(5)
$\mathbf{r}^u(\mathbf{u}, d) = \text{div}\boldsymbol{\sigma}(\mathbf{u}, d) + \mathbf{b} = \mathbf{0}$ $r^\varphi(\mathbf{u}, d) = Y(\mathbf{u}, d) - \kappa(d) - \text{div}\mathbf{Y}(d) \quad \dot{r}^d(\dot{d}) = \dot{d}$	
<p>(1) Balance of Linear Momentum, (2) Kuhn-Tucker Conditions, (3) Additional Completeness and Non-Overlapping Requirements, (4) Elastic Solution Domain, (5) Damaged Solution Domain</p>	

**Table 2.** *Strong Form of the Coupled Problem*

### 4. Weak form of the coupled problem

As a prerequisite for a finite element discretization the coupled nonlinear boundary value problem has to be reformulated in weak form. Therefore, the equations in strong form are tested by the corresponding virtual quantities to render the virtual work expression, see Table 3.

Note that the decomposition of the solution domain  $\mathcal{B}$  into an active damaged and an inactive elastic domain  $\mathcal{B} = \mathcal{B}^d \cup \mathcal{B}^e$  and  $\emptyset = \mathcal{B}^e \cap \mathcal{B}^d$  is indeed a quite implicit definition at this stage since one has to test for all possible combinations of

$$G^u(\mathbf{u}, d; \delta \mathbf{u}) = 0 \quad \forall \delta \mathbf{u} \quad (1)$$

$$G^\varphi(\mathbf{u}, d; \delta d) \leq 0 \quad \dot{G}^d(\dot{d}; \delta \varphi) \geq 0 \quad \forall \delta d, \delta \varphi > 0 \quad (2)$$

$$\mathcal{B} = \mathcal{B}^e \cup \mathcal{B}^d \quad \text{and} \quad \emptyset = \mathcal{B}^e \cap \mathcal{B}^d \quad (3)$$

$$\mathcal{B}^e = \{\mathbf{x} \in \mathcal{B} \mid G^\varphi \leq 0, \dot{G}^d = 0 \quad \forall \delta d, \delta \varphi > 0 \text{ in } \mathcal{B}^e\} \quad (4)$$

$$\mathcal{B}^d = \{\mathbf{x} \in \mathcal{B} \mid G^\varphi = 0, \dot{G}^d > 0 \quad \forall \delta d, \delta \varphi > 0 \text{ in } \mathcal{B}^d\} \quad (5)$$

$$G^u(\mathbf{u}, d; \delta \mathbf{u}) = \int_{\partial \mathcal{B}^t} \delta \mathbf{u} \cdot \mathbf{t}^p \, dA + \int_{\mathcal{B}} [\delta \mathbf{u} \cdot \mathbf{b} - \nabla_x \delta \mathbf{u} : \boldsymbol{\sigma}(\mathbf{u}, d)] \, dV$$

$$G^\varphi(\mathbf{u}, d; \delta d) = \int_{\mathcal{B}} [\delta d [Y(\mathbf{u}, d) - \kappa(d)] + \nabla \delta d \cdot \mathbf{Y}(d)] \, dV$$

$$\dot{G}^d(\dot{d}; \delta \varphi) = \int_{\mathcal{B}} \delta \varphi \dot{d} \, dV$$

(1) Weak Form of Balance of Linear Momentum, (2) Weak Form of Kuhn-Tucker Conditions, (3) Additional Completeness and Non-Overlapping Requirements, (4) Elastic Solution Domain, (5) Damaged Solution Domain

**Table 3.** Weak Form of the Coupled Problem

supports with all admissible test functions. Furthermore, it is remarkably that the above decomposition corresponds to the pointwise complementary condition  $\dot{d}\varphi = 0$ .

## 5. Discretized form of the coupled problem

The above set of equations has to be discretized in time and space, whereby we apply without loss of generality the implicit Euler backward method and resort to the standard Bubnov-Galerkin finite element method. Then the temporal integration of the primary variables  $\mathbf{u}$  and  $d$  renders a discretized temporal update for the values  $\mathbf{u}_{n+1}$  and  $d_{n+1}$ . Furthermore, based on the iso-parametric concept, the displacement field  $\mathbf{u}^h|_{\mathcal{B}_e} = \sum_k N_x^k \mathbf{u}_k \in H_1(\mathcal{B})$  together with its variation  $\delta \mathbf{u}^h|_{\mathcal{B}_e} = \sum_k N_x^k \delta \mathbf{u}_k \in H_1^0(\mathcal{B})$  is elementwise expanded in terms of the nodal values  $\mathbf{u}_k$  and  $\delta \mathbf{u}_k$  by the same shape functions as the geometry  $\mathbf{x}^h|_{\mathcal{B}_e} = \sum_k N_x^k \mathbf{x}_k$ . Moreover, the damage field  $d^h|_{\mathcal{B}_e} = \sum_k N_d^k d_k \in H_1(\mathcal{B})$  together with its variation  $\delta d^h|_{\mathcal{B}_e} = \sum_k N_d^k \delta d_k \in H_1(\mathcal{B})$  is elementwise expanded by independent shape functions in terms of the nodal values  $d_k$  and  $\delta d_k$ . Likewise, the test function  $\delta \varphi|_{\mathcal{B}_e} = \sum_k N_d^k \delta \varphi_k \in L_2(\mathcal{B})$  is discretized by the same shape functions as for the damage field in terms of nodal

values  $\delta\varphi_k$ . The corresponding discrete algorithmic equations of the coupled problem are given in Table 4.

$R_K^u(\mathbf{u}_{n+1}^h, d_{n+1}^h) = \mathbf{0} \quad \forall K \text{ in } \mathbb{B}$	(1)
$R_K^\varphi(\mathbf{u}_{n+1}^h, d_{n+1}^h) \leq 0 \quad \Delta R_K^d(d_{n+1}^h) \geq 0 \quad \forall K \text{ in } \mathbb{B}$	(2)
$\mathbb{B} = \mathbb{B}_{n+1}^d \cup \mathbb{B}_{n+1}^e \quad \text{and} \quad \emptyset = \mathbb{B}_{n+1}^d \cap \mathbb{B}_{n+1}^e$	(3)
$\mathbb{B}_{n+1}^e = \{K \in \mathbb{B} \mid R_K^\varphi \leq 0, \Delta R_K^d = 0\}$	(4)
$\mathbb{B}_{n+1}^d = \{K \in \mathbb{B} \mid R_K^\varphi = 0, \Delta R_K^d > 0\}$	(5)
$R_K^u = \mathbf{A}_e \int_{\partial B_e \cap \partial B^t} N_x^k t_{n+1}^p \, dA + \int_{B_e} [N_x^k \mathbf{b}_{n+1} - \nabla_x N_x^k \cdot \boldsymbol{\sigma}(\mathbf{u}_{n+1}^h, d_{n+1}^h)] \, dV$	
$R_K^\varphi = \mathbf{A}_e \int_{B_e} [N_d^k [Y(\mathbf{u}_{n+1}^h, d_{n+1}^h) - \kappa(d_{n+1}^h)] + \nabla_x N_d^k \cdot \mathbf{Y}(d_{n+1}^h)] \, dV$	
$\Delta R_K^d = \mathbf{A}_e \int_{B_e} [N_d^k [d_{n+1}^h - d_n^h]] \, dV$	
<p>(1) Discrete Algorithmic Balance of Linear Momentum, (2) Discrete Algorithmic Kuhn-Tucker Conditions, (3) Additional Completeness and Non-Overlapping Conditions, (4) Discrete Algorithmic Elastic Solution Domain, (5) Discrete Algorithmic Damaged Solution Domain</p>	

**Table 4.** Discretized Form of the Coupled Problem

Note that now the discrete algorithmic decomposition of the node point set is indeed a complete explicit definition since one only has to check separately all node points  $K \in \mathbb{B}$ . Furthermore it is remarkably that the above discrete algorithmic decomposition corresponds to the discrete algorithmic complementary condition  $\Delta R_K^d R_K^\varphi = 0 \quad \forall K \text{ in } \mathbb{B}$ .

The initially unknown decomposition of the discretization node point set into active and inactive subsets  $\mathbb{B} = \mathbb{B}_{n+1}^d \cup \mathbb{B}_{n+1}^e$  at time step  $t_{n+1}$  is determined iteratively by an active set search. Thereby, the strategy is borrowed from convex nonlinear programming as is frequently used e.g. in multi-surface and crystal plasticity.

An efficient algorithm for the solution of the coupled problem stated in the above sections is offered by a monolithic iterative strategy. Here, the discrete algorithmic balance of linear momentum together with the discrete algorithmic Kuhn-Tucker conditions are solved simultaneously within a typical Newton-Raphson scheme.

## 6. Constitutive update

Typically, a strain-driven constitutive update algorithm has to provide the updated dependent variables, like stress, damage flux, etc. at time  $t_{n+1}$ , moreover its consistent linearization is essential in order to set up the appropriate global iteration matrix for the quadratically converging global Newton-Raphson strategy.

The constitutive update of the simplest geometrically linear damage prototype model for given  $\epsilon_{n+1}$ ,  $d_{n+1}$  is summarized in Table 5. Note that despite its implicit character the constitutive update does not rely on local iterations usually employed in standard update algorithms.

$\sigma_{n+1}$	$=$	$[1 - d_{n+1}] \mathbf{E}_\epsilon : \epsilon_{n+1}$	(1)
$\tilde{\sigma}_{n+1}$	$=$	$\mathbf{E}_\epsilon : \epsilon_{n+1}$	(2)
$\mathbf{Y}_{n+1}$	$=$	$-c \mathbf{d}_{n+1}$	(3)
$Y_{n+1}$	$=$	$\frac{1}{2} \epsilon_{n+1} : \mathbf{E}_\epsilon : \epsilon_{n+1}$	(4)
$\kappa_{n+1}$	$=$	$\phi^{-1}(d_{n+1}) = \kappa_0 - \frac{1}{h} \ln(1 - d_{n+1})$	(5)
(1) Nominal Stress, (2) Effective Stress, (3) Damage Flux, (4) Local Energy Release Rate, (5) Internal Variable Update			

**Table 5.** Update Algorithm for Gradient Damage

Note that the damage variable  $d$  is a given input for the update of the internal variable  $\kappa$ . Thereby, for convenience of exposition we use here a simple exponential-type evolution law for the damage evolution, which allows a closed form update for the internal variable  $\kappa$ . Otherwise, an additional local iteration for  $\kappa = \phi^{-1}(d)$  would become necessary but does not limit the generality of the formulation proposed here. It is remarkable that the linearization of the constitutive update, i.e. the tangent operator results in a symmetric global iteration matrix.

Note that the update algorithm in the local case varies significantly. Here, only the strains  $\epsilon_{n+1}$  are given and in a first step the local energy release rate  $Y_{n+1}$  is computed. Based on this the history variable  $\kappa_{n+1}$  is determined from the maximum of the new

local energy release rate  $Y_{n+1}$ , the old value  $\kappa_n$  or the initial damage threshold  $\kappa_0$ , respectively. Finally, the updated damage variable  $d_{n+1}$  is computed from the new history variable  $\kappa_{n+1}$ . Thus in contrast to the gradient update algorithm the damage variable  $d$  is a dependent variable in the local case.

## 7. Examples

In the above sections the theory as well as the numerics were outlined for a gradient damage formulation. This is now applied to computational examples showing the performance of the elaborated model by modifying the gradient parameter as well as discretization density in deterioration processes.

### 7.1. One-dimensional bar under uniaxial tension

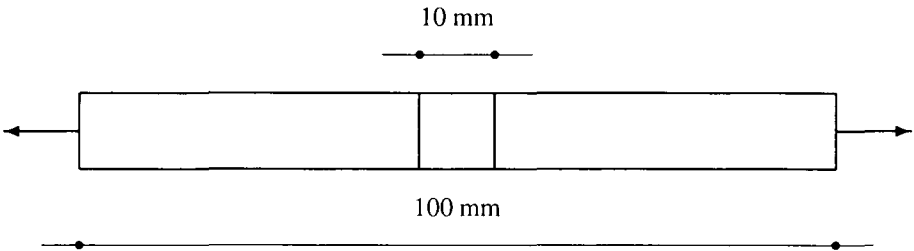


**Figure 1.** 1-D-Model Problem: Bar under Uniaxial Tension

As a model problem we will examine in the sequel the bar in Fig. 1 under uniaxial tension for the sake of demonstration. The problem statement, which includes a slight material imperfection in the middle of the bar, is taken from Peerlings, de Borst, Brekelmans & de Vree [PEE 96], whereby homogeneous Neumann boundary conditions for the damage flux were prescribed at the boundary. The material is modeled based on a linear elastic gradient damage formulation with a simple exponential-type evolution law for the damage evolution. The material parameters for the following examples are summarized in Table 6.

The total bar is discretized with 80, 160, 320, 640, 1280 and 2560 elements. Thereby, due to the symmetry in the problem statement only one half of the bar is considered. The load is applied using arclength control enabling to trace the post-peak branch of the load-deflection curves. The main objective is to show the performance of the gradient model. Therefore as a comparison, the local model is also addressed. For different possibilities of discretization techniques for the local and quasi-local case we refer to Liebe and Steinmann [LIE 01]. Likewise, a two-field finite element formulation for elasticity coupled to local damage was proposed by Florez-Lopez et. al [FLO 94]. In this work, we focus on the classical approach in local damage with

$E = 10000.00 \text{ N/mm}^2$	(1)
$E_r = 9000.00 \text{ N/mm}^2$	(2)
$\kappa_0 = 0.01 \text{ N/mm}^2$	(3)
$h = 0.01$	(4)

(1) Elastic Modulus, (2) Reduced Elastic Modulus, (3) Initial Damage Threshold, (4) Exponential Hardening Modulus

**Table 6.** *Material Parameters*

linear element expansions for the displacement. Hereby, the local damage variable field is not separately discretized. The element type for gradient damage reflects a continuous expansion in both the displacement as well as the damage variable field. Hereby, it appears that the choice of linear expansions in both discretized fields yields the most effective and efficient results. This can be explained by considering the discretized Kuhn-Tucker conditions, which seem to be mainly affected by the choice of discretization order. Using quadratic expansions for the displacements renders piecewise linear strains and would result in a quadratic expansion of the elastically stored energy  $Y$ . This quantity would then be coupled with a highly nonlinear history variable expression  $\kappa$  and a piecewise constant damage gradient, which causes oscillations in both the damage variable distribution as well as in the load-deflection curves. Therefore, we use linear-linear approximations ( $P^01P^01$ ) for the following examples in gradient damage, which give stable results. The different element formulations are described in Table 7.

Damage For- mulation	Discretization Variable	Continuity of Ap- proximation	Element Type
local	$\mathbf{u}$	$C^0$	$P^01$ Expansion
gradient	$\mathbf{u}, d$	$C^0/C^0$	$P^01P^01$ Expansion

**Table 7.** *Classification of Element Formulations*

Firstly, as a reference for the gradient model we investigate the local damage case. Here, in order to trigger localization we additionally introduced a graded imperfection in the middle of the bar. Hereby, the first element has the lowest elastic modulus and the neighboring elements a slightly increased elastic modulus  $E_g = 9500.0 \text{ N/mm}^2$  compared to the rest of the bar elements with the highest elastic modulus. The re-

sulting load-deflection curves for the classical local  $P^0$ 1 element type are displayed in Fig. 2. The typical deficiency in terms of a quasi-lack of convergence in the post-peak branch of the curves can be observed upon mesh refinement. This is even more emphasized in Fig. 3 depicting the corresponding distribution of the damage variable, whereby a concentration of damage evolution is accumulated in only one element.

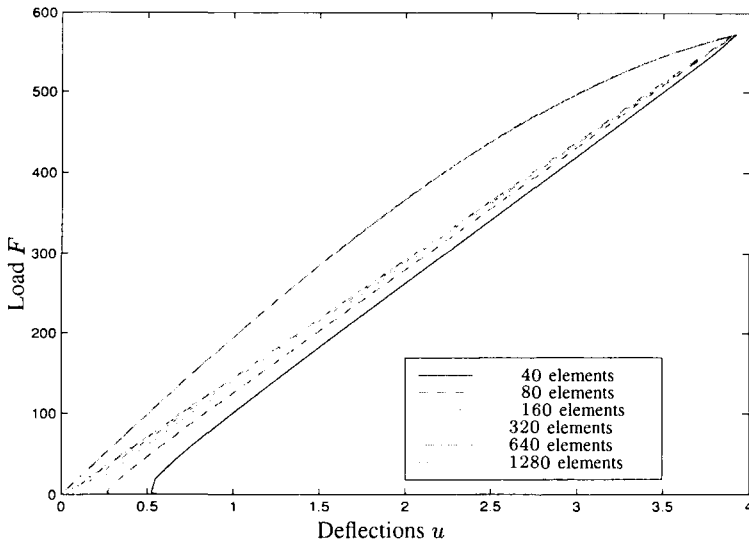


**Figure 2.** Load versus Deflection ( $P^0_1$ )

Secondly, to overcome the lack of discretization invariance the following examples are based on the incorporation of the gradient regularization in the constitutive model as described in the previous sections. First we show the quasi-mesh independence for a constant gradient parameter  $c = 100.0$  upon mesh densification, see Fig. 4 and Fig. 5. Clearly, also for different gradient parameters the solution converges upon mesh densification. Thereby, higher values of the gradient parameter render a somewhat more ductile post-peak behavior, see Fig. 6 and Fig. 7. In any case, the corresponding distribution of the localized zone is convergent.

Note that the influence of modifying the gradient parameter results in a variation of ductility in the load-deflection curves, see Fig. 6 as well as in the damage variable distribution, see Fig. 7. Hereby, the regularizing effect of the incorporation of gradients into the damage model is obvious as the jumps in the damage variable distribution in the local model are smoothed out in the gradient one. Nevertheless, the overall solution shows a shrinkage of the localized band width upon further loading into a crack line mode, i.e. a gradual transition from a damaged zone into a line crack.

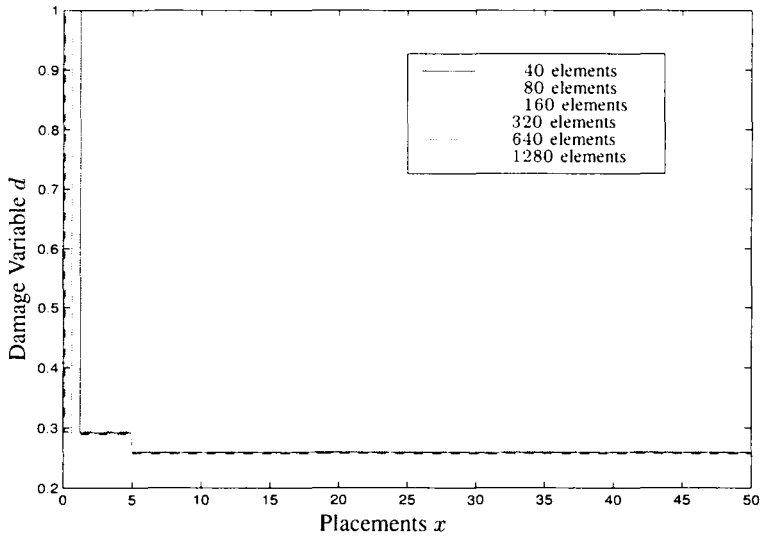


**Figure 3.** Damage Variable Distribution ( $P^0_1$ )

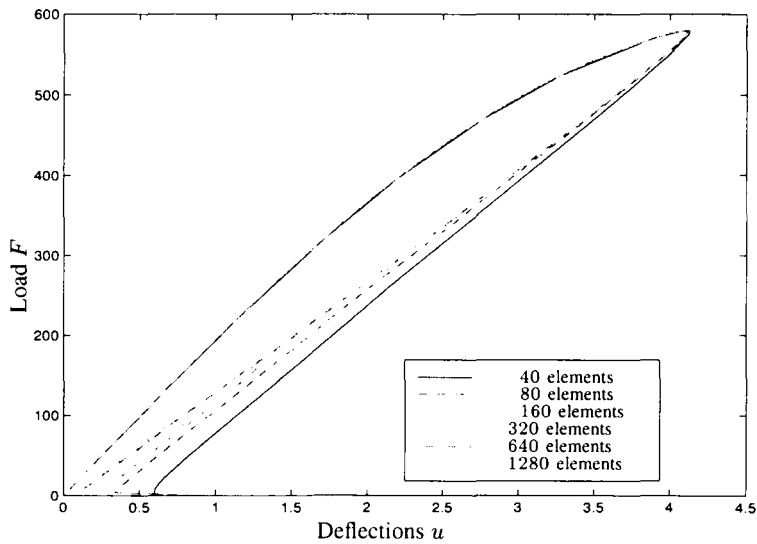


**Figure 4.** Load versus Deflection for  $c = 100.0$  ( $P^0_1 P^0_1$ )

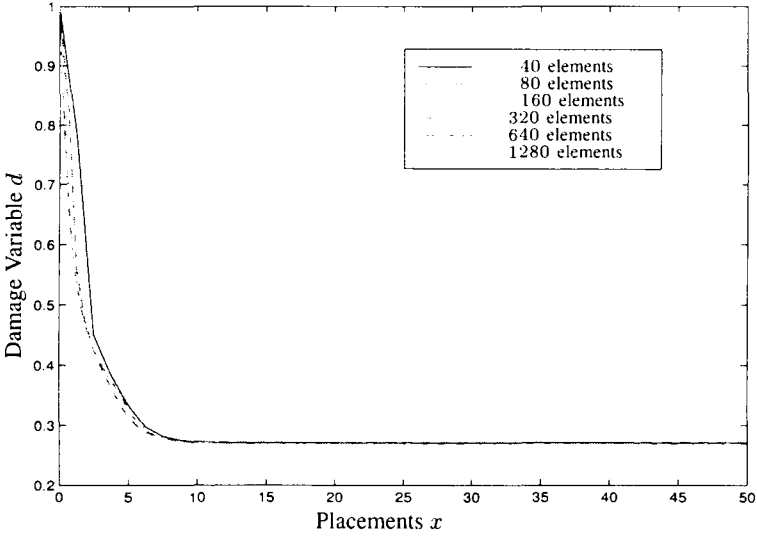


**Figure 5.** Damage Variable Distribution for  $c = 100.0 (P^0_1P^0_1)$

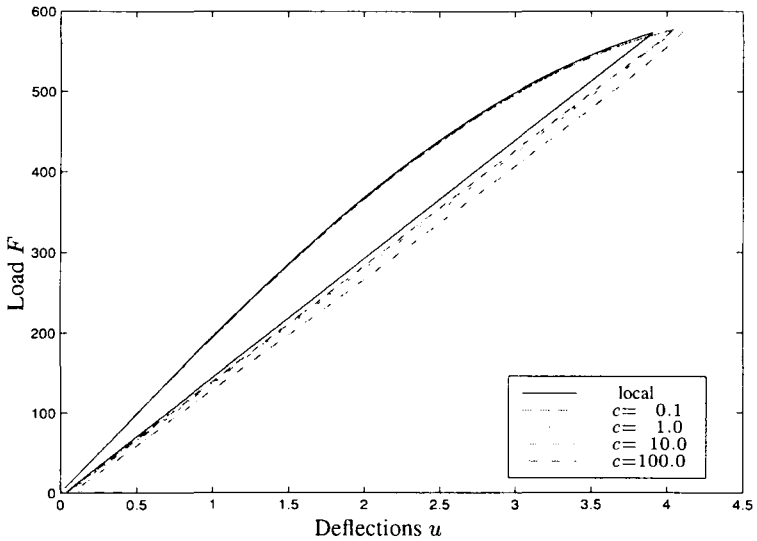


**Figure 6.** Load versus Deflection for constant mesh discretization (640 elements) and varied  $c = 0.0, 0.1, 1.0, 10.0, 100.0$

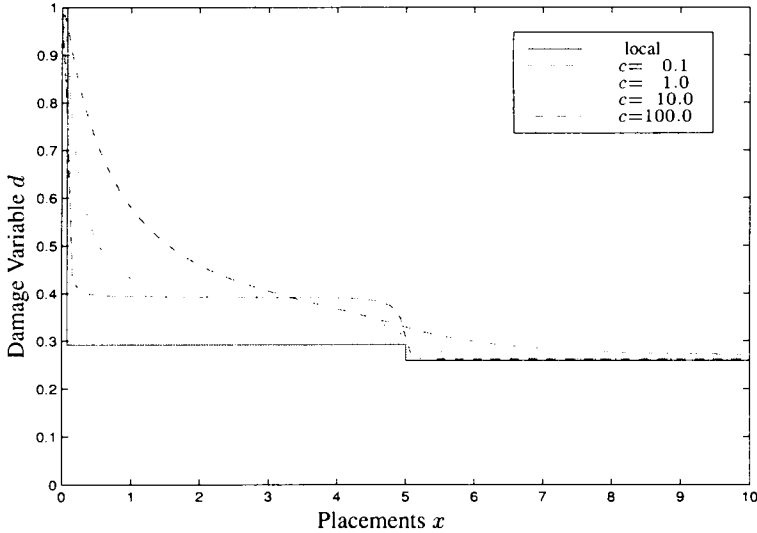


**Figure 7.** Damage Variable Distribution for constant mesh discretization (640 elements) and varied  $c = 0.0, 0.1, 1.0, 10.0, 100.0$

## 7.2. Two-dimensional panel under uniaxial tension

Finally, in order to show the performance of the damage gradient formulation in 2d we investigate the panel in Fig. 8 under tension. Again we have included a slight material imperfection in the center elements. The material is modeled in analogy to the 1d example, see Table 6. The bar is discretized with  $20 \times 10$  and  $40 \times 20$  Q1Q1-elements (continuous approximation of both displacement field and damage field). Again, we focus here on the damage variable distribution which emphasizes the convergent performance of the gradient damage formulation as displayed in Fig. 9 and Fig. 10.

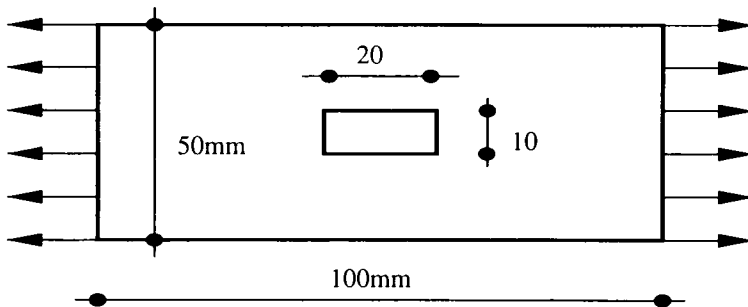


**Figure 8.** 2-D-Model Problem: Panel with Center-Imperfection

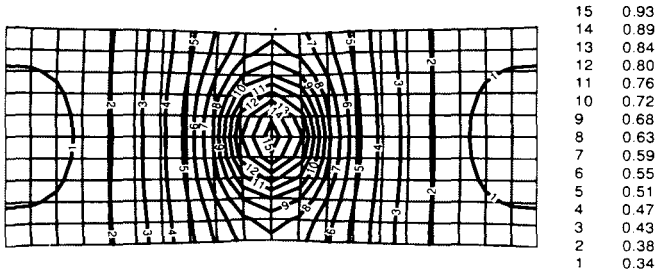


**Figure 9.** *Damage Distribution shortly before reaching  $d=1$ ,  $c=100$ , coarse mesh*

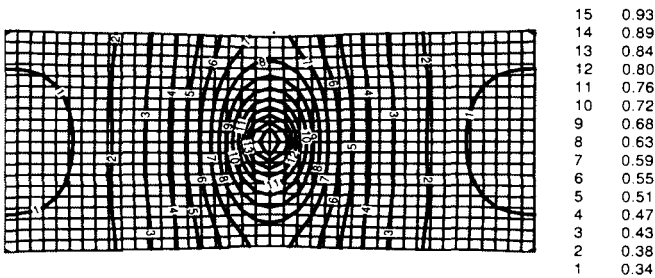


**Figure 10.** *Damage Distribution shortly before reaching  $d=1$ ,  $c=100$ , fine mesh*

## 8. Conclusion

We have derived a theoretical formulation and the corresponding discretized algorithmic format of a gradient damage model. Based on a positive domain dissipation and the postulate of maximum dissipation we end up with algorithmic Kuhn-Tucker conditions in dependence on the quasi-nonlocal energy release rate, which is conjugated to the damage evolution. On the numerical side, due to this special structure, an active set search becomes necessary for the monolithic iterative solution of the coupled problem within a typical Newton-Raphson strategy. Nevertheless only standard FE-data structures and corresponding FE-modules are involved. Moreover, we end up with a symmetric iteration matrix avoiding the use of a secant stiffness matrix as typ-

ically adopted in nonlocal models. In addition to that, other gradient damage models usually result in a non-symmetric tangent operator, see e.g. Peerlings et al. [PEE 96].

Considering a model problem of an one-dimensional bar under uniaxial tension we firstly investigated the classical local element formulation with only continuous element expansions for the displacement. Here, the local theory resulted in spurious mesh dependence in particular for the damage variable distribution. This could only be remedied by using the gradient formulation with gradient parameters  $c > 0$ . For verification we investigated the behavior for  $c = 1.0, 10.0, 100.0$ . Thereby, it could be noted that with increasing gradient parameter the solution becomes somewhat more ductile. In any case, mesh densification renders mesh objective results and convergent distributions of the damage variable field in both 1d as well as 2d computations. It is remarkable, that a gradual transition from a damaged zone into a line crack can be observed in the load-deflection curves in contrast to standard gradient models.

Therefore, it was emphasized that based on the theory and numerics underlying the gradient model advocated here, the regularization effect in damage is considerable. Moreover, the simultaneous solution of the discrete algorithmic Kuhn-Tucker conditions in addition to the discretized algorithmic balance of linear momentum offers an elegant solution strategy in the numerical treatment of gradient damage. In particular it is notable that the additional discrete algorithmic loading and unloading conditions complemented by an active set search are implemented on a nodal basis, which is in contrast to alternative gradient-enhanced formulations.

## 9. References

- [BEN 93] BENALLAL, A., BILLARDON, R. AND GEYMONAT, G. «Bifurcation and localization in rate-independent materials: some general considerations». In *CISM Lecture Notes N° 327*, pages 1–44. Springer-Verlag, 1993.
- [BEN 95] BENALLAL, A. AND TVERGAARD, V. «Nonlocal continuum effects on bifurcation in the plane strain tension-compression test». *J. Mech. Phys. Solids*, 43:741–770, 1995.
- [BOR 96a] DE BORST, R., BENALLAL, A. AND HEERES, O. «A gradient-enhanced damage approach to fracture». *J. Phys. IV*, 6:491–502, 1996.
- [BOR 96b] DE BORST, R. AND PAMIN, J. «Some novel developments in finite element procedures for gradient-dependent plasticity and finite elements». *Int. J. Num. Meth. Eng.*, 39:2477–2505, 1996.
- [COM 96] COMI, C. «A gradient damage model for dynamic localization problems». *Rend. Sc. Istituto Lombardo*, A 130:119–141, 1996.
- [COM 99] COMI, C. «Computational modelling of gradient-enhanced damage in quasi-brittle materials». *Mech. Cohes.-Frict. Mater.*, 4:17–36, 1999.

- [FLO 94] FLOREZ-LOPEZ, J., BENALLAL, A., GEYMONAT, G. AND BILLARDON, R. «A two-field finite element formulation for elasticity coupled to damage». *Comp. Meth. Appl. Mech. Eng.*, 114:193–212, 1994.
- [LIE 01] LIEBE, T. AND STEINMANN, P. «Theory and numerics of a thermodynamically consistent framework for geometrically linear gradient plasticity». *Int. J. Num. Meth. Eng.*, in press 2001.
- [MEN 00] MENZEL, A. AND STEINMANN, P. «On the continuum formulation of higher gradient plasticity for single and polycrystals». *J. Mech. Phys. Solids*, 48:1777–1796, 2000.
- [PAM 94] PAMIN, J. «Gradient-dependent plasticity in numerical simulation of localization phenomena». Diss., Delft University of Technology, 1994.
- [PEE 96] PEERLINGS, R., DE BORST, R., BREKELMANS, W. AND DE VREE, J. «Gradient enhanced damage for quasi-brittle materials». *Int. J. Num. Meth. Eng.*, 39:3391–3403, 1996.
- [POL 98] POLIZZOTTO, C. AND BORINO, G. «A thermodynamics-based formulation of gradient-dependent plasticity». *Eur. J. Mech. A/Solids*, 17:741–761, 1998.
- [SLU 93] SLUYS, L., DE BORST, R. AND MUEHLHAUS, H. «Wave propagation, localization and dispersion in a gradient-dependent medium». *Int. J. Solids Struct.*, 30:1153–1171, 1993.
- [STE 96] STEINMANN, P. «Views on multiplicative elastoplasticity and the continuum theory of dislocations». *Int. J. Eng. Sci.*, 34:1717–1735, 1996.
- [STE 99] STEINMANN, P. «Formulation and computation of geometrically non-linear gradient damage». *Int. J. Num. Meth. Eng.*, 46:757–779, 1999.